Journal of Nuclear Materials 384 (2009) 330–335

Contents lists available at ScienceDirect

Journal of Nuclear Materials

journal homepage: www.elsevier.com/locate/jnucmat

Letter to the Editor

Transformation kinetics of zirconium alloys under non-isothermal conditions

A.R. Massih *

Quantum Technologies AB, Uppsala Science Park, Uppsala SE-75183, Malmö University, SE-205 06 Malmö, Sweden

ARTICLE INFO

Article history:
Received 29 September 2008
Accepted 28 November 2008

ABSTRACT

The overall solid-to-solid phase transformation kinetics under non-isothermal conditions in Zr alloys has been evaluated using a model presented on our preceding note [1]. It uses as input an applied thermal history and calculates the time/temperature variation of the volume fraction of the new phase in $\alpha \leftrightarrow \beta$ transition in Zr alloys under heating/cooling, in concordance with experiments.

1. Introduction

The light-water reactors that make up most of world's nuclear energy (electricity) today use Zr-base alloys for structural components and fuel cladding [2]. Fabrication of fuel cladding tube commonly comprises heat treatments (temperature range of roughly 300–1300 K) that involve time-dependent phase transformation of Zr alloy from hexagonal (α-phase) to cubic (β-phase) crystal structure [3,4]. Similarly, under extreme in-service conditions, e.g., during a postulated loss-of-coolant accident (LOCA), fuel cladding will be subjected to a rapid increase in temperature (up to 1000–1500 K) in steam environment, which not only induces $\alpha \rightarrow \beta$ transformations, but also leads to rapid oxidation of Zr and hydrogen uptake, until the reactor core gets reflooded by water and cladding is quenched to α-phase [5]. Kinetics of phase transformation affects the microstructure, hence material characteristics of the final product on fabrication. It is also pivotal for the assessment of the mechanical properties essential for fuel rod integrity (deformation and burst) during a postulated LOCA.

The crucial parameter for the transformation kinetics is the evolution of the volume fraction of the new phase as a function of time and temperature under temperature loads which occur in non-isothermal conditions. Empirical-based methods have been used in the past to simulate Zr-alloy phase transformations under LOCA conditions [6,7]. More recent modelling efforts are the works of Forgeron et al. [8] and Brachet et al. [9] and the implementation of such models in a fuel performance code [10].

In this letter, we employ a method for calculation of the volume fraction of the favoured phase in Zr alloys as a function of time and temperature during phase transformation in non-isothermal conditions. It is a sequel to our previous paper, which focused on the theoretical aspects of the considered model [1].

2. Experimental data on zirconium alloys

We make a short survey of experiments reported in literature pertinent for the application of our model to zirconium base alloys. These experiments also provide data for model verification. We consider the kinetics of phase transformation of Zircaloy-4 (Zr–1.5Sn–0.2Fe–0.1Cr–0.12O, by wt%) and Zr1%Nb (Zr–1.0Nb–0.12O, by wt%). Zirconium in solid state undergoes an allotropic transformation from the low temperature hexagonal closed-packed (hcp) α-phase to body-centered cubic (bcc) β-phase at 1138 K [2]. On cooling, the transformation is either bainitic or martensitic depending on the cooling rate, with a strong epitaxy of the α-platelets in the former β grains [2].

Solid state phase equilibria of Zircaloy-4 have been investigated experimentally by Miquet et al. [11], who reported a prevalence of four phase domains: $\alpha + \chi$ up to 1081 K, $\alpha + \beta + \chi$ from 1081 to 1118 K, $\alpha + \beta$ between 1118 and 1281 K, and β-phase above 1118 K. Here, χ refers to the intermetallic hexagonal Laves phase $Zr(Fe,Cr)_2$, see e.g. [12]. Quenching Zircaloy from β-phase in moderate cooling rates produces two variants of Widmanstätten structure, namely, the basketweave and the parallel-plate structure [13,3]. However, at cooling rates greater than 1000 K s^{-1} a martensite structure is observed, while for very low cooling rates, $\leqslant$0.5 K s^{-1}, the needle-shaped structure is rarely seen [14].

The equilibrium phase transformation properties of Zr–Nb–O alloys have recently been surveyed and evaluated in [15]. Hunt and Niessen [16,17] have investigated the continuous cooling transformation behaviour of Zr–Nb–O alloys in the composition range of 0.5–5.7 wt%Nb and 0.14–0.53 wt%O. They identified nucleation and growth reactions due to the formation of α-Zr at the β-grain boundaries and the transformation $\beta_{Zr} \rightarrow \alpha_{Zr} + \beta_{Nb}$ throughout the grains. Increasing the niobium content slowed the phase transformation both at the grain-boundaries and in the bulk. On the other hand, increasing oxygen raised the temperature of both reactions, causing intergranular nucleation to occur earlier and intragranular nucleation to occur later.

---

* Tel.: +46 18509690.
E-mail address: alma@quantumtech.se

0022-3115/$ - see front matter © 2008 Elsevier B.V. All rights reserved.
doi:10.1016/j.jnucmat.2008.11.033

Toffolon et al. [18] have examined the influence of oxygen content on $\alpha/(\alpha+\beta)$ and $(\alpha+\beta)/\beta$ transition temperatures in Zr1%Nb employing calorimetry. Their data indicate that increasing the oxygen content, from about 0.1 wt% to 0.27 wt%, will increase the $(\alpha+\beta)/\beta$ transition temperature from 1185 K to 1265 K, while the $\alpha/(\alpha+\beta)$ temperature varies in the range of 900–910 K. They also studied the influence of niobium content in the range of 0.5–2.5 wt% in Zr alloys containing 0.12-0.13 wt% oxygen. They observed that raising the niobium content lowers both the $(\alpha+\beta)/\beta$ temperature (by about 15 K) and the $\alpha/(\alpha+\beta)$ transition temperature, where the latter remains constant for Nb contents $\geqslant 1$ wt%.

The overall $\alpha \leftrightarrow \beta$ transition in Zircaloy-4 has been studied by a number of workers in the past [19–24] and more recently in [8,9], which include also experiments on Zr1%Nb (M5$^{\text{TM}}$) alloy and the effects of hydrogen on phase transformation behaviour. Forgeron et al. [8] studied $\alpha \leftrightarrow \beta$ transition of the Zr alloys by determining both their equilibrium (steady-state) temperature-dependence and their transient behaviour, with respect to the fraction of volume transformed, for the heating/cooling rates from ±0.1 to ±100 K s^{-1}. More specifically, they determined the equilibrium behaviour of α/β-phase fraction as a function of temperature by means of calorimetry measurements. They used low heating/cooling rates from 0.1 K/min to 20 K/min. Moreover, they carried out direct measurements of the α/β-phase fraction by employing image analysis techniques on samples annealed for a few hours at different temperatures then quenched to room temperature. For kinetic measurements, they made use of dilatometric equipment, where thermal cycles were applied on tubular samples, 12 mm in length, in vacuum or helium gas. According to Forgeron et al. [8], the uncertainty of the relative phase fraction in calorimetric measurements was less than 5%.

In a subsequent paper, Brachet et al. [9] extended Forgeron et al.'s work in order to investigate the influence of hydrogen content on the kinetics of $\alpha \leftrightarrow \beta$ transformation.[1] Their results under quasi-equilibrium conditions indicate that hydrogen expedites the phase transition, i.e., the transition from α- to the $(\alpha+\beta)$-domain starts at lower temperature with increasing hydrogen content. The hydride precipitation/dissolution temperatures, i.e., the inverse solubility limit for hydrogen in Zircaloy-4 and Zr1%Nb alloy under the same kinetic condition have been determined by Brachet et al. [9]. Their results for the precipitation temperature as a function of hydrogen concentration at a cooling rate of 0.167 Ks^{-1} indicate that Zr1%Nb alloy has a lower precipitation temperature than Zircaloy-4 for hydrogen concentrations less than 700 wppm. The effect of hydrogen on the $\alpha \leftrightarrow \beta$ phase transformation in Zircaloy-4 versus Zr1%Nb alloy was also alluded by Brachet et al. (2002). They displayed plots of $\alpha/(\alpha+\beta)/\beta$ phase transformation temperatures of Zircaloy-4 and Zr1%Nb alloy as a decreasing function of hydrogen for heating rate of 10 Ks^{-1}, with Zr1%Nb alloy transition temperatures remaining below that of Zircaloy-4 at most by around 30 K.

3. The model

We denote the transformed volume fraction by variable y, which is a function of time t and temperature T with the property $0 \leqslant y \leqslant 1$. Following [1,25], we consider that y is not too far from its steady-state or equilibrium value $y_s(T)$ at a given temperature T, and write

$$\frac{dy}{dt} = \frac{y_s(T) - y}{\tau_c(T)}, \tag{1}$$

where τ_c is a characteristic time of phase transformation. Note that Eq. (1) is controlled by two external temperature-dependent functions, i.e., $\tau_c(T)$ and $y_s(T)$, with $y_s(T)$ being the fraction of a new phase formed at temperature T after infinitely long time and $0 \leqslant y_s(T) \leqslant 1$. Both these functions are material specific temperature-dependent quantities and can be deduced from experimental data on properties of a particular material or derived from appropriate models verified with such data as has been done below. Under non-isothermal conditions, the temperature follows a path which may be an arbitrary function of time, and hence Eq. (1) needs to be solved numerically.

For computation of y as function of time and temperature, the two functions $y_s(T)$ and $\tau_c(T)$, which appear in Eq. (1), need to be specified. Let us first consider the former. The experimental data for the temperature dependence of steady-state volume fraction under phase transition suggest that $y_s(T)$ has an S-shaped or sigmoid form. For this reason, we have selected for the $\alpha \leftrightarrow \beta$ transition in Zr alloys a relation of the form

$$y_s = \frac{1}{2}\left[1 - \tanh\left(\frac{T - T_{cent}}{T_{span}}\right)\right], \tag{2}$$

for the equilibrium β-phase volume fraction at temperature T. Here, T_{cent} and T_{span} are material specific parameters related to the center and the span of the mixed-phase temperature region, respectively. They are determined from the measured phase boundary temperatures T_α and T_β through

$$T_{cent} = \frac{T_\alpha + T_\beta}{2}; \qquad T_{span} = \frac{T_\beta - T_{cent}}{2.3}. \tag{3}$$

Here, T_α and T_β are defined as the temperatures that correspond to 99% α- and β-phase fractions, respectively.

The relation for $\tau_c(T)$ or its inverse, the rate parameter $k = \tau_c^{-1}$, in general, depends on both the nucleation rate and growth rate of the new phase, which are strongly temperature dependent. It is usual to adopt an Arrhenius-type relation for the rate parameter (see [1] and references therein)

$$k(T) = k_0 \exp\left[-\frac{E}{k_B T(t)}\right], \tag{4}$$

where k_0 is a kinetic prefactor, E the overall effective activation energy and k_B the Boltzmann constant. Here, E is an effective activation energy, which combines the activation energies of nucleation and growth. Rationalization of this combined effect is discussed in [26,27]. The material-dependent parameters in relations (2) and (4) for Zircaloy-4 and Zr1%Nb alloy are identified in Appendix A. In addition, the temperatures for the onset of phase transitions for $\alpha \to \alpha+\beta$ and $\beta \to \beta+\alpha$ are material-dependent quantities which are stated in detail in Appendix A. These quantities are heating/cooling rate ($Q = \mathrm{d}T/\mathrm{d}t$) dependent which have been taken into account in our formulation.

4. Computations

We first depict and compare the temperature dependence of the equilibrium volume fraction of the transformed phase for Zircaloy-4 and Zr1%Nb alloy using Eq. (2). Fig. 1 (top) shows this comparison. It is the plot of Eq. (2) or the solution of Eq. (1) at very low heat ratings ($Q < 0.1$ Ks^{-1}). The symbols represent experimental data [8]. It can be seen that the considered correlations fit the data pretty well. Moreover, we note that the transition temperature for Zr1%Nb occurs at a lower temperature and also the volume of the transformed phase shifts to lower temperature (niobium is a β-phase stabilizer). The effect of hydrogen on phase transformation of Zircaloy-4 is shown in Fig. 1 (bottom). The results are in agreement with experimental data of Brachet et al. [9]. Again, we observe that as hydrogen concentration is increased, the $\alpha \to \alpha+\beta$

---

[1] Hydrogen is absorbed in Zr alloys during normal in-reactor service, mainly as a result of oxidation.

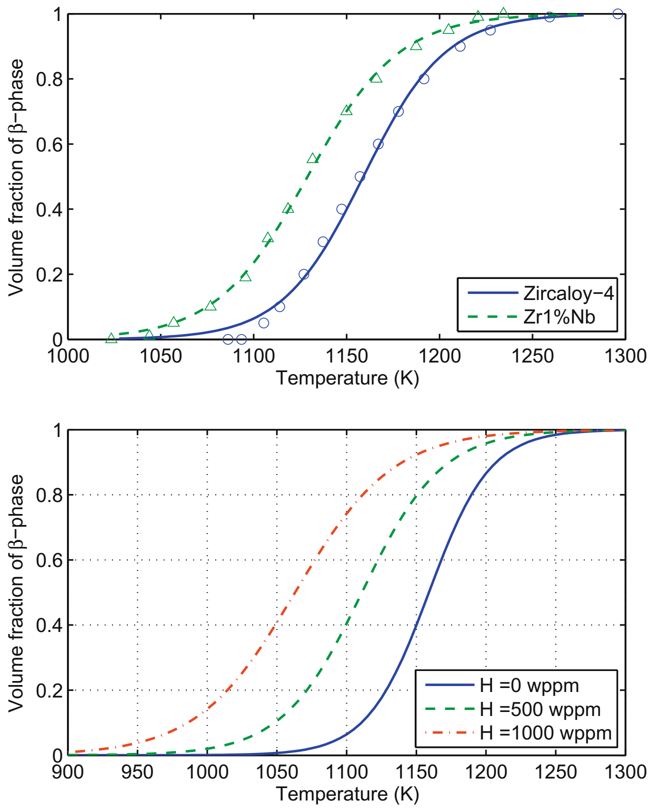

Fig. 1. Equilibrium volume fraction of β-phase as a function of temperature. (Top) Comparison between Zircaloy-4 and Zr1%Nb alloy. The symbols represent measured data [8]. (Bottom) Influence of hydrogen in Zircaloy-4 on phase transformation, see ref. [9].

transition temperature is lowered and the volume fraction of the favoured phase is shifted to lower temperatures.

For non-isothermal conditions Eq. (1), with the initial conditions $y(0) = 0$ on heating and $y(0) = 1$ on cooling, is used in order to calculate the volume reaction of β-phase as a function of temperature. The Runge–Kutta method of order 4 and 5 [28] was used to integrate Eq. (1). The effect of heat rating Q on the fraction of the transformed phase for Zircaloy-4 under heating/cooling is shown in Fig. 2. The symbols denote the measurement points while the lines are calculations according to the aforementioned model. The corresponding calculations and data for Zr1%Nb subject to heating are shown in Fig. 3. Hence, as $|Q|$ is increased, the transformed volume fraction shifts to higher/lower temperatures under heating/cooling, respectively.

5. Discussion

The method utilized here to calculate the volume fraction of the favoured phase as a function of time and temperature can be applied to any input thermal history since we solve Eq. (1) numerically. The question that may arise is how well this approximate equation compares with the prevailing exactly solved models in isothermal conditions. Integrating Eq. (1) gives

$$y/y_s = 1 - \exp\left(-\int_{t_0}^{t} k[T(s)]ds\right), \tag{5}$$

with $k = \tau_c^{-1}$. For isothermal conditions, Eq. (5) yields

$$y/y_s = 1 - e^{-k(t-t_0)}, \tag{6}$$

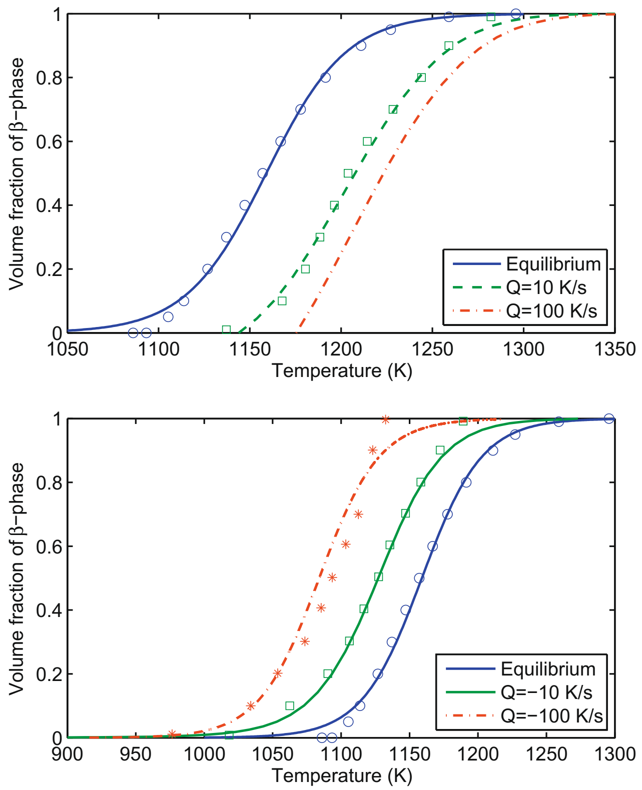

Fig. 2. Volume fraction of β-phase as a function of temperature for Zircaloy-4 at different heating/cooling rates (top/bottom); the symbols represent measured data [8].

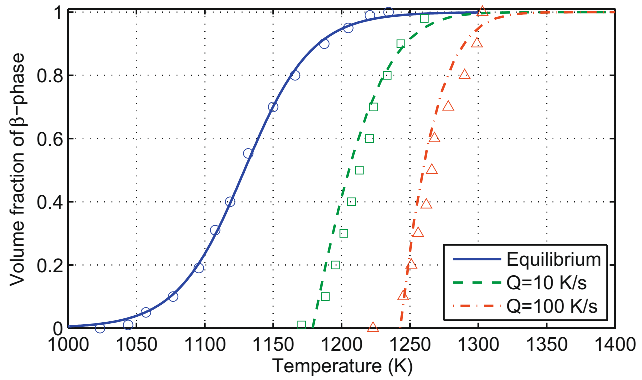

Fig. 3. Volume fraction of β-phase as a function of temperature for Zr1%Nb alloy at different heating rates, the symbols represent measured data [8].

where t_0 is the incubation time for the onset of phase transformation. This relation is a special case of the Avrami model [29,30] related to site saturation transformation on grain surfaces under isothermal conditions with Avrami's exponent $m = 1$.[2] Moreover, as has been shown by Cahn [30], equation of form (6) is theoretically exact for the systems in which the nucleation rate is sufficiently rapid such that site saturation occurs early in the reaction period, see ref. [1] for a more detailed discussion.

This type of model has been used in the past to describe β(bcc)-to-α(hcp) phase transition in Zr–2.5 wt%Nb under isothermal conditions [31] and in Ti–6 wt%Al–2 wt%V, e.g. [32], where Widmanstätten side-plates form during continuous cooling. More specifically, Higgins and Banks [31] measurements on

---

[2] $f = 1 - \exp(-kt^m)$, where $f = y/y_s$ is the degree of transformation.

Zr–2.5 wt%Nb at an isothermal temperature of 1076 K showed that $m \approx 0.95$, which is close to the theoretical value of $m = 1$. Likewise, experiments by Holt on Zircaloy-4 under continuous cooling (in the temperature range of 1123–1203 K) show that $m \approx 0.9$ [19,20]. Similarly, our data analysis of the experimental work of [24] on Zircaloy-4 at temperatures 1163 K and 1223 K indicate that $m \approx 0.93$. Hence, the model we have used in our analysis has a sound theoretical basis (the nucleation rate is high and site saturation occurs early during reaction) for describing the overall phase transformation of Zr alloys in the temperature range of interest (1100–1300 K).

Comparing now our model with the early approach of Holt et al. [7], which was also used later by Brachet et al. [9], we note that Holt et al.'s approach is merely an ad-hoc formula with virtually no theoretical justification. It expresses the volume fraction rate (of the new phase) directly to the temperature deviation from equilibrium with a power dependence ($\propto |T_{eq} - T|^{2.5}$, where T_{eq} is the equilibrium temperature of the new phase). Whereas, Eqs. (1) and (5) rest on the generic theory of solid-to-solid phase transformation [33] and is related to the diffusion-limited precipitation of the new phase on grain boundaries [1].

We should point out that our model, as it stands, is not applicable to Zr1%Nb alloy under $\beta \to (\beta + \alpha)$ phase transition under pertinent cooling rates. This is because we have not found analogous data in literature, as presented in Fig. 2(b), for Zr1%Nb alloy to compare the model with. It has been reported that, cooling from β-phase even at low cooling rates (down to 0.1 Ks^{-1}), some Nb-enriched β-Zr in a metastable state is retained in the α-domain at room temperature [34]. Furthermore, Shebaldov et al. [34] point out that β-quenching Zr1%Nb at cooling rates greater than 80 Ks^{-1}, the alloy transforms by a diffusionless mechanism (martensitic transformation) to an hcp (α') structure. For cooling rates below 80 Ks^{-1}, the presence of Nb-enriched β-Zr may be due to a slow diffusion of Nb in Zr matrix which affects the full reversibility of $\beta \leftrightarrow \alpha$ transition [18]. This phenomenon may be modelled phenomenologically by altering (increasing) the characteristic time constant τ_c of the phase transition. To do this, however, experimental data for Zr1%Nb, as in Fig. 2(b), are needed.

The rate dependence of phase transformation stems from the fact that both nucleation and growth of a new phase are strongly temperature dependent mechanisms. Especially, the nucleation rate is a transient entity, and there is an associated delay time until it reaches its steady-state value [33]. So as the temperature rate is increased under heating, nucleation occurs less rapidly, requiring a higher temperature for formation of a new phase. This phenomenon is manifested in the start temperature for phase transition. In literature, the start temperature of first order phase transition has been related to the temperature dependence of the incubation time for nucleation. For example, Zhu and Devletian [35] studied the equilibrium and heating/cooling rate dependence of certain Zr and Ti alloys. Using differential thermal analysis experiments, they found that as the cooling rate is increased, the phase transition temperature ($T_{\beta \to \beta + \alpha}$) is reduced, whereas on heating ($T_{\alpha \to \alpha + \beta}$) the situation is converse. Building on the theoretical work of Russell [36] on heterogeneous nucleation, in particular the incubation time for nucleation on grain boundaries, Zhu and Devletian [35] obtained a relationship for the start of phase transformation when the heating/cooling rate Q is constant, in the form

$$\int_{T_0}^{T_s} (T - T_0)^2 \, T^{-1} e^{-E_b/k_B T} dT = CQ, \tag{7}$$

where T_s is the temperature at which the first critical nucleus is formed, T_0 the equilibrium transition temperature, E_b the activation energy for boundary diffusion of the involved elements in parent phase, and C is a constant.

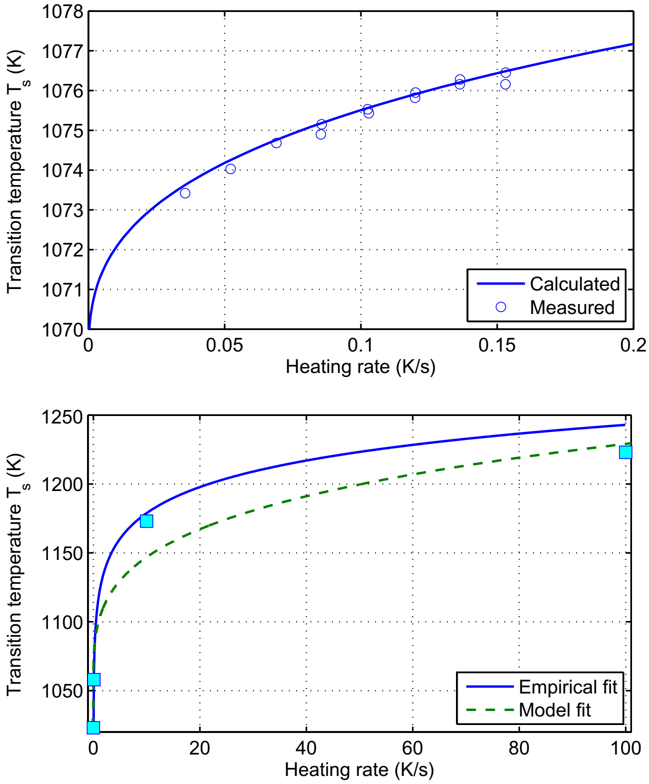

Fig. 4. Onset of $\alpha \to \alpha + \beta$ phase transition temperature versus heating rate: (Top) Zr–Fe alloy, calculated according to Eq. (B.3) versus measured data in [35]; (Bottom) Zr1%Nb alloy, where the model fit is based on Eq. (B.3), while the empirical fit is relation (A.3); the square symbols denote measurements [8].

Zhu and Devletian [35] experiments were carried out at very low heating/cooling rates ($|Q| < 0.4$ K/s) for the alloys examined. For some experimental Zr alloys, Zr–Fe and Zr–Fe–O, they found that $E_b/k_B \approx 9900$ K. We have noted that with a choice of $C = 8.5 \times 10^{-5}$ Ks, Eq. (7) fit their data on phase transition temperature vs. heating rate for Zr–Fe alloy excellently (Fig. 4 top), see the underlying calculations presented in Appendix B. However, when we naively extrapolated the calculations to heating rates of 0.1–100 K/s (with the same model parameters), the change in the $\alpha \to \alpha + \beta$ transition temperature was appreciably underestimated compared to the data presented in [8] for Zr1%Nb alloy. Fig. 4 (bottom) shows the results of calculations, according to Eq. (B.3), with $C = 3.68 \times 10^{-3}$ Ks and the measured data on Zr1%Nb alloy [8]. Also in this figure, the empirical relation Eq. (A.3) is depicted as a function of heating rate. Obviously, more data points are needed to ascertain the consistency of the model (and/or its selected parameters) or the reliability of the empirical power law.

We should mention that prudence needs to be exercised when applying the aforementioned models out of their experimental range of validity, that is for a given material and for particular metallurgical (grain size, microstructure) conditions. Nevertheless, the model for the overall phase transformation of the Zr alloys presented in this note captures the available data adequately. Thus, it can be used in predictive computer codes for the type of materials and conditions evaluated in this paper, when analyzing cladding behaviour under high temperature transients.

Acknowledgement

I am thankful to Tero Manngård and anonymous reviewers for their incisive comments on the manuscript. The work was sup-

Table 1
Parameters in Eq. (2) used for calculation of the equilibrium phase transformation.

Material	T_{cent} (K)	T_{span} (K)	Data source
Zircaloy-4	1159	44	[8]
Zr1%Nb	1129	49	[8]

ported by the Swedish Radiation Safety Authority under the Contract No. SKI2007/611, 200806001.

Appendix A. Material-dependent model parameters

The material-dependent parameters in our model for phase transformation are summarized in this appendix. We start by specifying the parameters T_{cent} and T_{span} appearing in Eq. (2) and in Table 1. The hydrogen concentration dependence of these quantities for Zircaloy-4 are: $T_{cent} = 1159 - 0.096w$ and $T_{span} = 44 + 0.026w$, where $0 \leqslant w \leqslant 1000$ wppm (weight parts per million hydrogen) based on the data presented in [9]. For the parameters in Eq. (4), we have used best fit values $k_0 = 60457 + 18129|Q|$ (s^{-1}) and $E/k_B = 16650$ (K), where $Q = \mathrm{d}T/\mathrm{d}t$ is the heat rate (Ks^{-1}) in the range $0.1 \leqslant |Q| \leqslant 100\ \mathrm{Ks}^{-1}$, for both Zircaloy-4 and Zr1%Nb alloy [1].

Regarding the starting temperature for the onset of phase transformation, experimental data on Zircaloy-4 and Zr1%Nb alloy indicate that this quantity is temperature rate dependent [8]. In our modeling of this effect, for Zircaloy-4, we have related the onset of $\alpha \to \alpha + \beta$ transformation temperature (heating) by fitting a power law relation to the experimental data reported in [8,9], which gave (in kelvin)

$$T_{\alpha\to\alpha+\beta} = \begin{cases} 1083 - 0.152w & \text{for} \quad 0 \leqslant Q < 0.1\ \text{K/s} \\ (1113 - 0.156w)Q^{0.0118} & \text{for} \quad 0.1 \leqslant Q \leqslant 100\ \text{K/s} \end{cases} \tag{A.1}$$

for $0 \leqslant w \leqslant 1000$ wppm. Also, a time (temperature) lag at the start temperature of phase transformation from $\beta \to \beta + \alpha$ is observed on cooling, which is not symmetric with the one on heating, i.e., from $\alpha \to \alpha + \beta$. Based on a few data points on Zircaloy-4 reported in [8,9], we estimate that (in kelvin)

$$T_{\beta\to\beta+\alpha} = \begin{cases} 1300 & \textit{for} \quad -0.1 < Q \leqslant 0\ \text{K/s} \\ 1302.8 - 8.333|Q|^{0.477} & \text{for} \quad -100 \leqslant Q \leqslant -0.1\ \text{K/s}. \end{cases} \tag{A.2}$$

Note that no hydrogen content dependent terms are included in Eq. (A.2), since no experimental data are reported in literature for Zircaloy-4 containing hydrogen under cooling. It is conceivable that a similar hydrogen concentration dependence as in Eq. (A.1) is in force under cooling. Similarly, for Zr1%Nb alloy, a best fit relation to the data reported in [9] under heating gives (in kelvin)

$$T_{\alpha\to\alpha+\beta} = \begin{cases} 1060 & \text{for} \quad 0 \leqslant Q < 0.1\ \text{K/s} \\ 1118Q^{0.023} & \text{for} \quad 0.1 \leqslant Q \leqslant 100\ \text{K/s}. \end{cases} \tag{A.3}$$

No data are reported in literature in the Q-range of interest for $T_{\beta\to\beta+\alpha}$ under cooling for the Zr1%Nb alloy. Nor we found experimental data on the effect of hydrogen for this alloy under heating/cooling in the Q-range of interest.

Appendix B. Calculation of start temperature for phase transition

Zhu and Devletian [35] using the classical nucleation theory à la Russell [36] found an effective field relation for the incubation (induction) time t_{inc} for nucleation in the form

$$t_{inc} = \frac{CT}{(T - T_0)^2}\exp(E_b/k_B T), \tag{B.1}$$

where T_0 is the equilibrium transition temperature, E_b the activation energy for boundary diffusion of the involved elements in the initial phase, and C is a constant. If the heating/cooling rate Q is constant, the additivity rule [33] for continuous heating/cooling is expressed in temperature space as

$$\int_{T_0}^{T_s} \frac{dT}{t_{inc}(T)} = Q, \tag{B.2}$$

where T_s is the temperature at which the first critical nucleus is formed. Substituting now Eq. (B.1) into Eq. (B.2), Eq. (7) of the text is obtained.

The integral in Eq. (7) can be evaluated by a simple change of variable $u = 1/T$ and making use of the general tabulated formula, or repeated partial integrations (see entry 2.324 in [37]) to obtain

$$\frac{e^{-q/T_s}}{2}\left[T_s(T_s - 4T_0 - q) - e^{q/T_s}(2T_0^2 + 4T_0 q + q^2)Ei\left(\frac{-q}{T_s}\right)\right] = CQ, \tag{B.3}$$

where $q \equiv E_b/k_B$ and $\mathrm{Ei}(\bullet)$ is the exponential integral defined by $Ei(z) = \int_{-z}^{\infty} dte^{-t}/t$ (for $z < 0$), where the principal value of the integral is taken, and evaluated in [38]. Eq. (B.3) can be solved for T_s as a function of Q for a given C, T_0 and q, the latter two quantities being material-dependent parameters.

As an example, for a Zr–Fe alloy, Zhu and Devletian [35], based on measurements carried out at very low heating rates ($|Q| < 0.2$ K/s), found that $T_0 = 1069$ K and $E_b/k_B \approx 9900$ K. Moreover, we have noted that with a choice of $C = 8.5 \times 10^{-5}$ Ks, Eq. (B.3) fit their data on the start phase transition temperature vs. heating rate for Zr–Fe alloy excellently, see Fig. 4 (top). For Zr1%Nb alloy using the data reported in [8] in the Q-range of 0.01 to 100 K/s (only four data points) we have found a best fit value of $C = 3.68 \times 10^{-3}$ Ks, using the aforementioned value for q and $T_0 = 1053$ K, see Fig. 4 (bottom).

References

[1] A.R. Massih, L.O. Jernkvist, Transformation kinetics of alloys under non-isothermal conditions, unpublished, preprint available from authors (September 2008).
[2] C. Lemaignan, A.T. Motta, in: R.W. Cahn, P. Haasen, E.J. Kramer (Eds.), Nuclear Materials, in: B.R.T. Frost (Ed.), Materials Science and Technology, vol. 10B, VCH, Weinheim, Germany, 1994, p. 1 (Chapter 7).
[3] A.R. Massih, T. Andersson, P. Witt, M. Dahlbäck, M. Limbäck, J. Nucl. Mater. 322 (2003) 138.
[4] A.R. Massih, L.O. Jernkvist, J. Phys. Chem. Solids 65 (2004) 1193.
[5] A.R. Massih, Review of experimental data for modelling LWR fuel cladding behaviour under loss of coolant accident conditions, Tech. Rep. 2007:14, Swedish Nuclear Power Inspectorate, Stockholm, Sweden (2007).
[6] H.M. Chung, A.M. Garde, T.F. Kassner, Mechanical properties of Zircaloy containing oxygen, Tech. Rep. ANL-77-10, Argonne National Laboratory (1976).
[7] R.A. Holt, H.E. Sills, S. Sagat, in: Fuel Element Performance Computer Modelling, No. 7 in IWGFPT, International Atomic Energy Agency, 1980, pp. 17–20, Specialists' Meeting, Blackpool, UK, 17–21 March 1980.
[8] T. Forgeron, J.C. Brachet, F. Barcelo, A. Castaing, J. Hivroz, J.P. Mardon, C. Bernaudat, in: G.P. Sabol, G.D. Moan (Eds.), Zirconium in the Nuclear Industry: Twelfth International Symposium, Vol. ASTM STP 1354, American Society for Testing and Materials, West Conshohocken, PA, USA, 2000, p. 256.
[9] J.C. Brachet, L. Portier, T. Forgeron, in: G.D. Moan, P. Rudling (Eds.), Zirconium in the Nuclear Industry: Thirteenth International Symposium, Vol. ASTM STP 1423, American Society for Testing and Materials, West Conshohocken, PA, USA, 2002, p. 673.
[10] P. Van Uffelen, C. Győri, A. Schubert, J. van de Laar, Z. Hózer, G. Spykman, J. Nucl. Mater. 383 (2008) 137.
[11] A. Miquet, D. Charquet, C.H. Allibert, J. Nucl. Mater. 105 (1982) 132.
[12] N.V. Bangaru, R.A. Busch, J.H. Schemel, in: R. Adamson, L. van Swam (Eds.), Zirconium in the Nuclear Industry: Seventh International Symposium, Vol. ASTM STP 939, American Society for Testing and Materials, Philadelphia, USA, 1987, p. 341.
[13] G. Ökvist, K. Källström, J. Nucl. Mater. 35 (1970) 316.
[14] D. Charquet, E. Alheritiere, in: R. Adamson, L. van Swam (Eds.), Zirconium in the Nuclear Industry: Seventh International Symposium, Vol. ASTM STP 939, American Society for Testing and Materials, Philadelphia, USA, 1987, p. 284.

[15] R.J. Peréz, A.R. Massih, J. Nucl. Mater. 360 (2007) 242.
[16] C.E.L. Hunt, P. Niessen, J. Nucl. Mater. 35 (1970) 134.
[17] C.E.L. Hunt, P. Niessen, J. Nucl. Mater. 38 (1971) 17.
[18] C. Toffolon, J.-C. Brachet, C. Servant, L. Legras, D. Charquet, P. Barberis, J.-P. Mardon, in: G. Moan, P. Rudling (Eds.), Zirconium in the Nuclear Industry: Thirteenth International Symposium, Vol. ASTM STP 1423, American Society for Testing and Materials, West Conshohocken, USA, 2002, p. 36.
[19] R.A. Holt, J. Nucl. Mater. 35 (1970) 322.
[20] R.A. Holt, J. Nucl. Mater. 47 (1973) 262.
[21] O.T. Woo, K. Tangri, J. Nucl. Mater. 79 (1979) 82.
[22] C.E.L. Hunt, E.M. Schulson, J. Nucl. Mater. 92 (1980) 184.
[23] M. Corchia, F. Righini, J. Nucl. Mater. 97 (1981) 137.
[24] J.S. Yoo, I.S. Kim, J. Nucl. Mater. 185 (1991) 87.
[25] J.B. Leblond, J. Devaux, Acta Met. 32 (1984) 137.
[26] A. Kempen, F. Sommer, E.J. Mittemeijer, J. Mater. Sci. 37 (2002) 1321.
[27] E.J. Mittemeijer, J. Mater. Sci. 27 (1992) 3977.
[28] A. Quarteroni, F. Saleri, Scientific Computing with MATLAB, Springer, Berlin, Germany, 2003.
[29] M. Avrami, J. Chem. Phys. 8 (1940) 212.
[30] J.W. Cahn, Acta Met. 4 (1956) 449.
[31] G.T. Higgins, E.E. Banks, Electrochem. Technol. 4 (1966) 341.
[32] B.K. Damkroger, G.R. Edwards, in: M. Anderson (Ed.), Simulation and Theory of Evolving Microstructures, The Minerals, Metals & Material Society, 1990, p. 129.
[33] J.W. Christian, The Theory of Transformations in Metals and Alloys, Pergamon, Amsterdam, 2002. part I.
[34] P.V. Shebaldov, M.M. Peregud, A.V. Nikulina, et al., in: G.P. Sabol, G.D. Moan (Eds.), Zirconium in the Nuclear Industry: Twelfth International Symposium, Vol. ASTM STP 1354, American Society for Testing and Materials, West Conshohocken, PA, USA, 2000, p. 545.
[35] Y.T. Zhu, J.H. Devletian, Met. Trans. A 22A (1991) 1993.
[36] K.C. Russell, in: H.I. Aaronson (Ed.), Phase Transformations, American Society for Metals, Metal Parks, Ohio, 1970, p. 219 (Chapter 6).
[37] I.S. Gradshteyn, I.M. Ryzhik, Tables of Integrals, Series, and Products, Academic Press, New York, 1980.
[38] M. Abramowitz, I.A. Stegun, Handbook of Mathematical Functions, Dover Publications, New York, 1964.